

An algorithm for transferring 2D arbitrary hp -refined finite element axially symmetric meshes to three dimensions

Maciej Paszyński ⁽¹⁾, David Pardo ⁽²⁾, Leszek Demkowicz ⁽³⁾, Carlos Torres-Verdin ⁽²⁾

⁽¹⁾ Department of Computer Science, AGH University of Science and Technology

⁽²⁾ Department of Petroleum Engineering, The University of Texas in Austin

⁽³⁾ Institute for Computational Engineering and Sciences, ICES, The University of Texas in Austin

Abstract

The 2D and 3D fully automatic hp adaptive Finite Element Method (FEM) codes generate a sequence of optimal hp refined meshes delivering exponential convergence rate of the numerical error with respect to the number of degrees of freedom (and CPU time). The optimal meshes are generated by performing a sequence of h or p refinements on the initial mesh. However, generation of optimal meshes in three dimensions is computationally expensive. We propose an algorithm for transferring of generated 2D optimal meshes into 3D meshes. The algorithm allows us to replace expensive 3D generation of optimal hp mesh by relatively inexpensive 2D generation of optimal meshes. The algorithm generates full revolution of the recorded optimal 2D mesh. The algorithm supports generation of either 3D axially symmetric meshes or non-axially symmetric tilted meshes. We apply that algorithm to perform a sequence of 3D DC borehole resistivity measurements simulations.

Keywords: Finite Element Method, DC resistivity borehole measurements, hp adaptivity

Motivation

Sequential and parallel 2D and 3D hp adaptive FEM codes (Demkowicz, 2002; Demkowicz & Pardo & Rachowicz, 2002; Paszyński & Kurtz, & Demkowicz, 2006; Kurtz, 2006; Paszyński & Demkowicz, 2006) generate in fully automatic mode a sequence of optimal FE meshes providing very accurate reliable solutions, with minimum size of the mesh (minimum number of degrees of freedom).

The codes start from an initial mesh, called *the coarse mesh*, with hexahedral elements and polynomial orders of approximations $p=2$ on elements edges, faces and interiors. The coarse mesh is then globally hp refined to produce *the fine mesh*, by breaking each element into 4 (in 2D) or 8 (in 3D) son elements, and increasing the polynomial order of approximation by one. The problem under consideration is solved on the coarse and on the fine mesh. The energy norm (H^1 Sobolev space norm) difference between coarse and fine mesh solutions is then utilized to estimate relative errors over coarse mesh elements. The optimal refinements are then selected and performed for coarse mesh elements with high relative error estimation. The coarse mesh elements are either broken into smaller son elements (this procedure is called h refinement, where h stands for the element size) or the polynomial order of approximation is increased on element edges, faces or interiors

(this procedure is called p refinement, where p stands for the element polynomial order of approximation). For each finite element from the coarse mesh we consider *locally* several possible h , p or hp refinements. For each finite element the refinement strategy providing maximum error decrease rate is selected. The error decrease rate

$$rate = \frac{\left\| u_{h/2, p+1} - u_{hp} \right\|_1 - \left\| u_{h/2, p+1} - w_{hp} \right\|_1}{nr dof \text{ added}} \quad (1)$$

is defined as relative error estimation in energy norm (H^1 Sobolev space norm) divided by number of degrees of freedom added. Here u_{hp} stands for the coarse mesh solution,

$u_{h/2, p+1}$ for the fine mesh solution and w_{hp} is the solution corresponding to proposed refinement strategy, obtained by the projection based interpolation technique

(Demkowicz, 2004). Thus, $\left\| u_{h/2, p+1} - u_{hp} \right\|_1$ is the relative error estimation over the current

coarse mesh finite element, and $\left\| u_{h/2, p+1} - w_{hp} \right\|_1$ is the relative error estimation for the

refinement strategy proposed for the finite element. The maximum error decrease rate means that we gain large error decrease rate by adding minimal number of degrees of freedom to the element under consideration. It should be emphasized that the decisions about optimal h , p or hp refinement can be made independently for each finite element from the coarse mesh.

The optimal mesh generated in such a way becomes a coarse mesh for the next iteration, and the entire procedure is repeated as long as the global relative error estimation is larger than the required accuracy of the solution (Demkowicz, 2002; Demkowicz & Pardo & Rachowicz, 2002 for more details). The most expensive part of that algorithm is the fine mesh solution. For 2D problems, the computational cost is relatively low, but the fine mesh solution for 3D problems is computationally expensive. To overcome the problem, fast iterative multi-grid solvers (Pardo & Demkowicz, 2006) or parallel computations (Paszyński & Kurtz & Demkowicz, 2006; Paszyński & Demkowicz, 2006) can be utilized. However, there is a class of 3D problems for which the 2D code can be utilized to generation of optimal mesh, and the 3D mesh can be obtained by transforming the generated 2D mesh into three dimensions. The class involves axially symmetric problems as well as problems obtained by tilting a 2D mesh, so the resulting 3D problem is no longer axially symmetric.

Problem under consideration

We will focus on DC resistivity logging applications, governed by Poisson equation

$$\nabla \cdot (\sigma \nabla u) = f \quad (2)$$

where u is a scalar potential of the electric field $E = -\nabla u$. The equation (2) results from 0 frequency Direct Current (DC) formulation of Maxwell's equations (Pardo & Demkowicz & Torres-Verdin & Paszynski, 2006).

The domain under consideration presented in figure 2 consists of four formation layers with different resistivities varying from 0.1 Ohm · m up to 100 Ohm · m. In the borehole with resistivity 0.2 Ohm · m there is one transmitter and three receiver electrodes. The

electrodes are modeled by assuming non-zero right-hand-side representing the imposed electric current. The height of domain is 200 meters, and the radius is 100 meters. The zero Dirichlet boundary conditions are assumed on the exterior of the cylindrical domain. The simulation requires a sequence of solutions of equation (2) for 80 different positions of transmitter and receiver electrodes. The electrodes are shifted along the borehole, and the values at the receiver electrodes are obtained from the FE solution for each new position. The estimation of the second vertical difference of potential at receiver electrodes is finally computed. This quantity is an approximation of

$$\frac{\partial^2 u}{\partial z^2} = \frac{\partial E}{\partial z} \quad (3)$$

which is physically expected to be sensitive to the resistivity of the formation. The goal of this simulation is to obtain this quantity for different vertical positions of the electrodes, the corresponding results are presented in figure 4. This is the forward model utilized during the inverse problem solution. The goal of the inverse modeling is to determine the location of the highly resistive oil formation in the ground.

The axially symmetric case presented in figure 2a is relatively simple to simulate. Of particular interest for industrial applications are more challenging problems with tilted formation layers, as presented in figure 2b-c, usually resulting from deviated wells. These problems are non-axially symmetric and require 3D simulations.

Mesh generation and conversion

To minimize the computational cost, we applied the 2D self-adaptive goal-oriented *hp* FEM code (Pardo & Demkowicz, 2006) to generate a 2D optimal mesh for the axially symmetric problem, presented in figure 2a. The initial mesh is presented in figure 1a. The resulting 2D *hp* refined mesh is presented in figure 3a. Various colors denote various polynomial orders of approximation. The generated 2D mesh is then transferred to the 3D software, by considering 4 or 8 second order elements in the azimuthal direction. The initial 3D mesh presented in figure 1b is obtained by full revolution of the initial 2D mesh, each 2D finite element has 4 corresponding 3D elements in this example.

The mapping between 2D and 3D elements is presented in figure 5. The *y* axis of the 3D element corresponds to the radial direction on the cylinder, the *x* axis of the 3D element corresponds to the azimuthal direction on the cylinder.

All *h* and *p* refinements generated during execution of *hp* adaptive 2D code are recorded. The following data are recorded for each refinement:

- Location of the initial mesh element being refined.
- Path on the refinement tree from initial mesh element to the active element being refined (since initial mesh elements are eventually broken into son elements, and new elements are recorded by using trees with roots located at initial mesh elements, see (Demkowicz & Pardo & Rachowicz, 2002) for more details).
- Type of refinement ('h' for *h* refinement, 'p' for *p* refinements).
- For *h* refinement, directions of 2D refinements ('1' for breaking 2D element in *x* direction, '10' for breaking 2D element in *y* direction, '11' for breaking 2D element in both directions).
- For *p* refinement, new polynomial order of approximation, and location of the element node being *p* refined (since *p* refinement concerns some element nodes, not the entire finite element).

The recorded 2D refinements are then read by the 3D code, and executed for all 4 finite elements corresponding to each 2D element.

1. For 2D h refinement in vertical direction (y 2D local direction), the top, left, bottom and right faces of 3D element must be broken into y local direction, see figure 6a.
2. For 2D h refinement in horizontal direction (x 2D local direction), the front, left, rear and right faces of 3D element must be broken into x local direction, see figure 6b.
3. p refinements of 2D finite element edges translate into p refinement of 3D finite element faces, compare figure 7, and p refinements of 2D finite element interior translate into p refinements of 3D finite element interior, however, various combination of orientations of both element must be considered:
 - p refinement of 2D element top edge translates into p refinement of 3D top face in 3D local x direction,
 - p refinement of 2D element bottom edge translates into p refinement of 3D bottom face in 3D local x direction,
 - p refinement of 2D element left-hand side edge translates into p refinement of 3D front face in 3D local y direction,
 - p refinement of 2D element right-hand side edge translates into p refinement of 3D top face in 3D local x direction,
 - p refinement of 2D element middle node in 2D local x direction translates into p refinement of interior of 3D element in 3D Y local direction
 - p refinement of 2D element middle node in 2D local y direction translates into p refinement of interior of 3D element in 3D Z local direction.

Execution of h refinements in 3D never breaks front and rear faces of 3D elements in vertical direction, since the problem is axially symmetric. Also, polynomial orders of approximation are never changed on left and right-hand side faces of 3D elements (on azimuthal direction faces). This is not recommended, since the hp refine mesh must fulfill the so-call *minimum rule: the orders of approximation on faces cannot be greater than the corresponding orders of approximation in adjacent elements interiors, and orders of approximation on edges cannot be greater than the corresponding orders of approximation on adjacent faces*. We enforce the above rule at the end of the 3D mesh conversion, by setting orders of approximation on faces as the minimum of the corresponding orders of interiors of adjacent elements, and orders of approximation on edges as the minimum of the corresponding orders of adjacent faces. This method do not slow down our refinement procedure, since the decision about optimal refinements are made locally, *only* for the element interiors. The orders of approximation on faces and edges must be adjusted to interior orders. In other words, order of approximation on faces cannot be larger then orders of approximation in adjacent elements interiors, because it will be not possible to extend the polynomials from face into adjacent interiors.

Results

The 2D mesh for the axially symmetric problem was converted into a 3D axially symmetric mesh. The parallel version of the 3D code (Paszyński & Demkowicz, 2006) was utilized to speedup the computations. The generated mesh was distributed into 8 processors, see figure 8. The problem (2) was solved for 80 positions of transmitter and receiver electrodes. The global p refinement was performed for each position, and the

problem was solved a second time over the mesh with polynomial order of approximation increased uniformly by 1, to verify the quality of the solution.

We computed the second difference of the potential in the vertical direction at the receiver electrodes. The obtained results are presented in figure 4a.

Then, the 3D mesh was tilted by 30, 45 and 60 degrees, and the entire procedure was repeated. There are very small differences between results obtained on the original converted 3D mesh and on the mesh with increased p , so the error of the numerical solution is negligible.

Conclusions

- The conversion of 2D optimal hp refined mesh into 3D mesh is a fast way to generate 3D optimal meshes.
- The results for the 3D axially symmetric problem as well as for tilted 3D mesh provide reliable accurate solution of the problem under consideration (Poisson equation governing DC borehole resistivity measurements).
- There are some problems where the results over tilted 3D converted mesh contain large error, e.g. DC resistivity measurements simulations for a borehole with steel casing (Pardo & Paszyński & Torres-Verdin & Demkowicz, 2006), where the solution contain more then 100% error. In such a case, the 3D mesh must be generated by using fully automatic hp adaptivity in three dimensions, which may take several days of single processor computations, or several hours of parallel computations (Paszyński & Pardo & Torres-Verdin & Demkowicz, 2006).

Acknowledgements

The work reported in this paper was partially supported by Polish MEiN grant no. 3 T08B 055 29, by the Foundation for Polish Science under program Homing, and by The University of Texas at Austin Research Consortium on Formation Evaluation, jointly sponsored by Aramco, Baker Atlas, BP, British Gas, ConocoPhillips, Chevron, ENI E&P, ExxonMobil, Halliburton Energy Services, Hydro, Marathon Oil Corporation, Mexican Institute for Petroleum, Occidental Petroleum Corporation, Petrobras, Schlumberger, Shell International E&P, Statoil, TOTAL, and Weatherford.

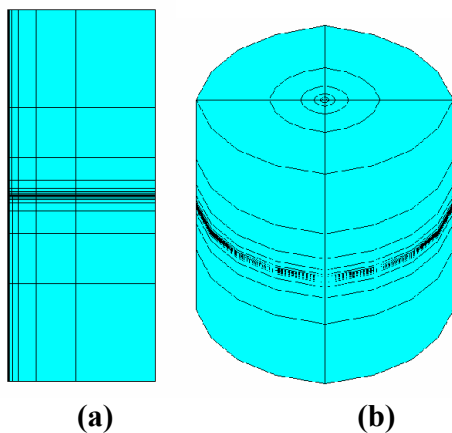


Figure 1 (a) The initial mesh for 2D goal-oriented hp adaptive FEM code. The polynomial order of approximation $p=2$ globally. (b) The initial mesh for 3D FEM code.

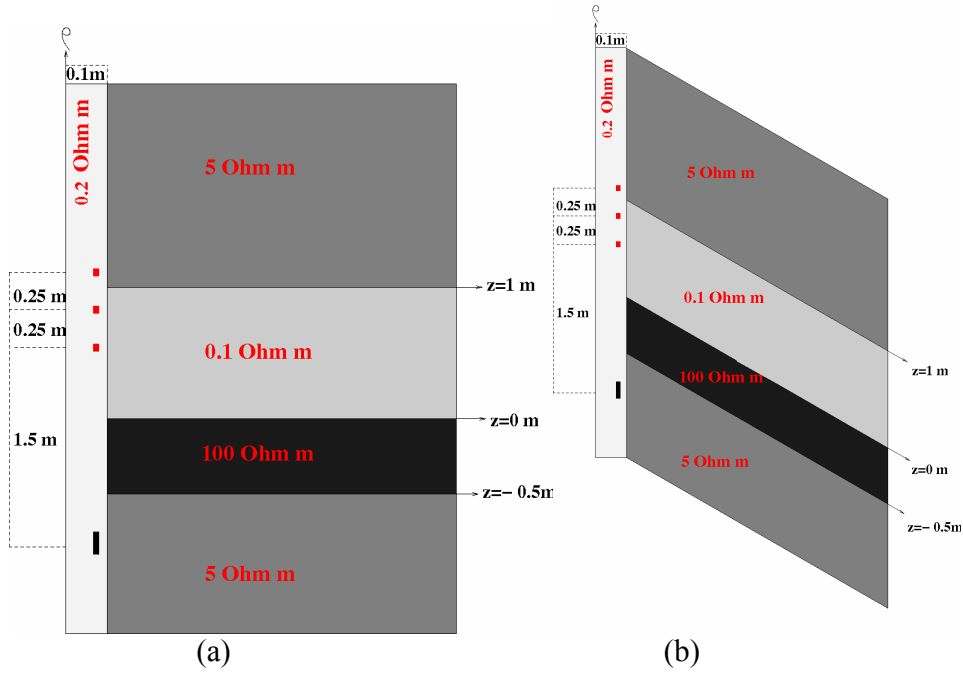


Figure 2. (a) The axisymmetric domain with a borehole, 1 transmitter and 3 receiver antennas, and formation layers with different resistivities. (b) The domain with formation layers tilted by 30 degrees.

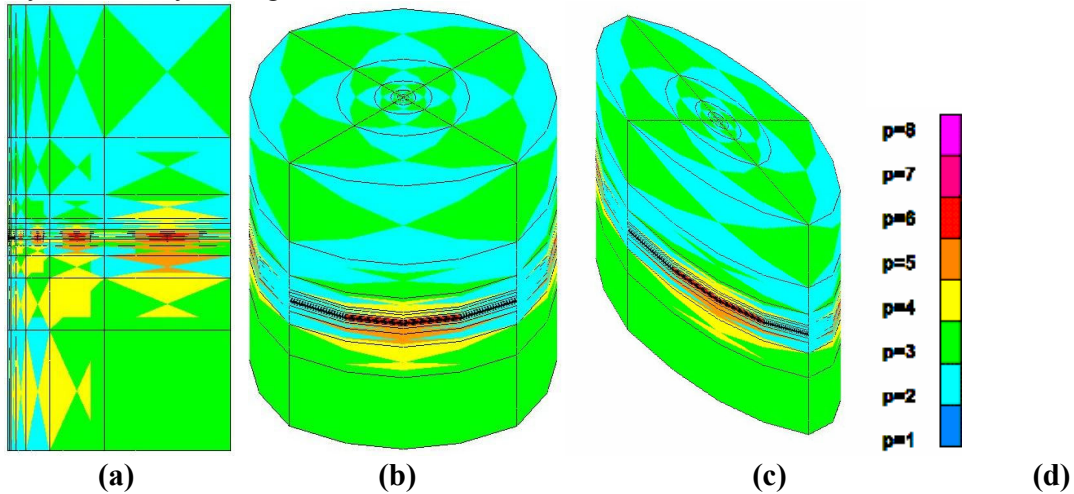


Figure 3 (a) The optimal mesh generated by using 2D goal-oriented hp adaptive FEM code. (b) The 3D optimal mesh obtained by conversion of the 2D mesh generated. (c) The optimal mesh was tilted by 30 degrees. (d) Polynomial orders of approximation varying from $p=1$ to $p=8$.

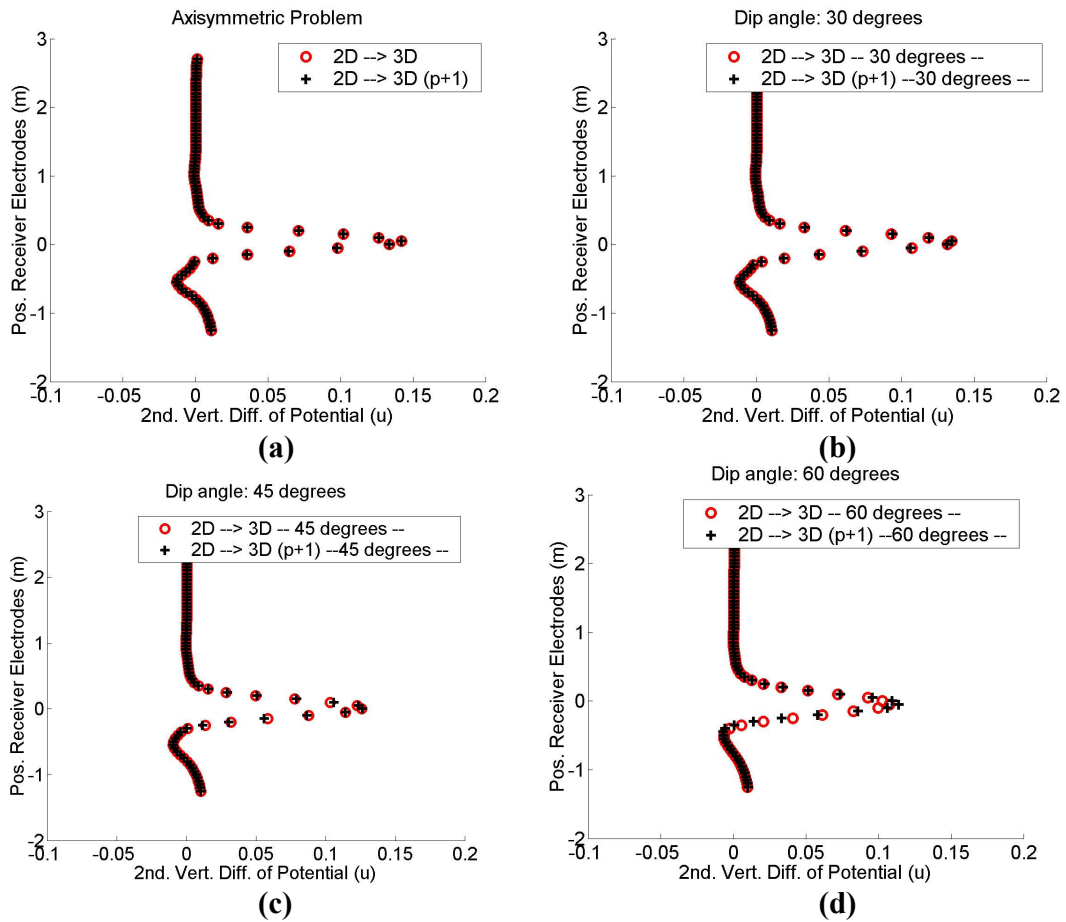


Figure 4 (a) DC resistivity measurements logging curves for axisymmetric case, (b) 30 degrees, (c) 45 degrees, (d) 60 degree deviated wells.

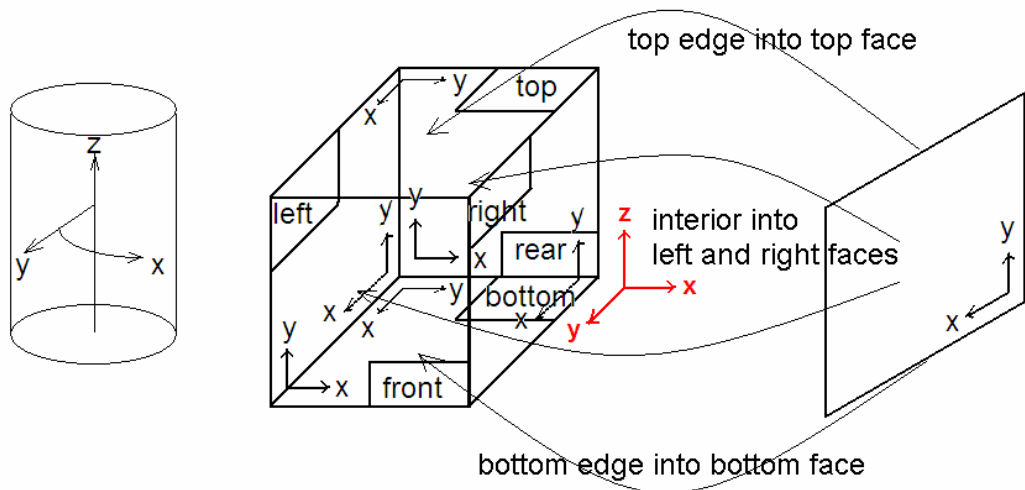


Figure 5 2D finite element is mapped onto 3D finite element. The top and bottom edges of 2D element are mapped into top and bottom faces of 3D element. The interior of 2D element is mapped into left and right faces of the 3D element. Various orientations of 2D and 3D element edges, faces and interiors must be taken into account during the mapping.

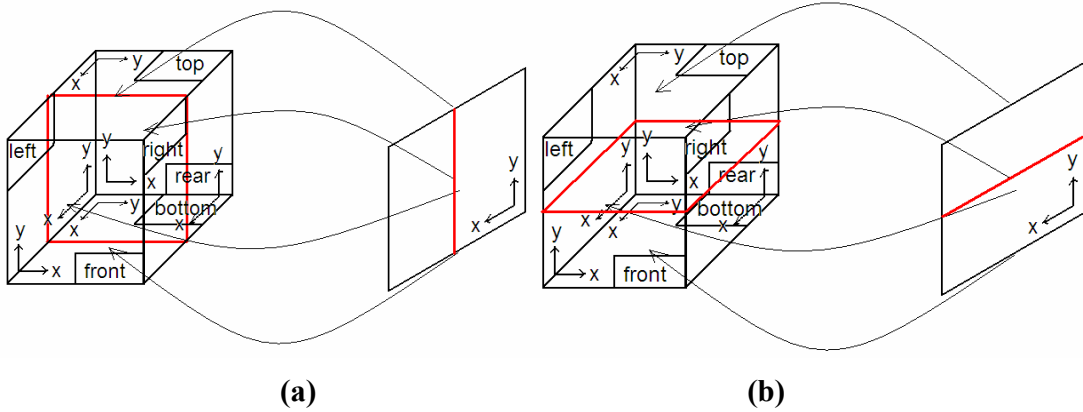


Figure 6. (a) Breaking of 2D element in x direction maps into breaking of bottom and top faces of 3D element in y direction and left and right faces in y directions. (b) Breaking of 2D element in y direction maps into breaking of left and right faces of 3D element in x direction and front and rear faces in x directions.

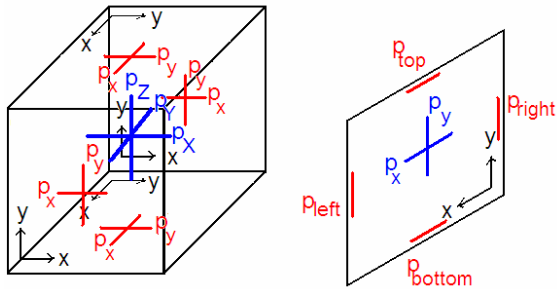


Figure 7 Polynomial orders of approximation on 2D finite element edges are mapped onto orders of approximation on 3D finite element faces. Polynomial orders of approximation on 2D finite element interior in x and y 2D local element directions are mapped into orders of approximation of interior of 3D finite element in local 3D y and z directions.

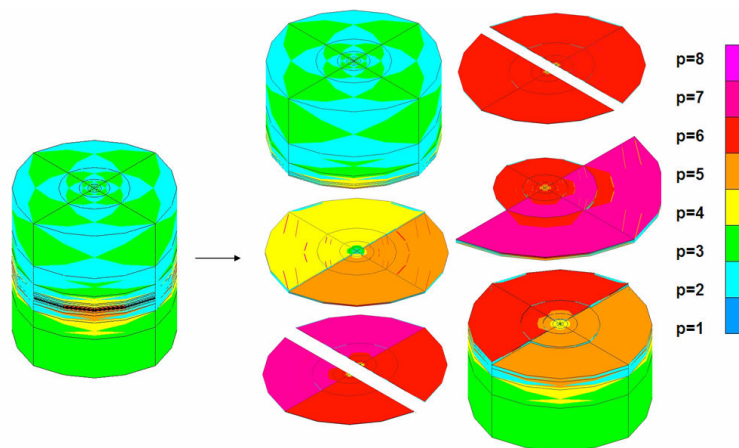


Figure 8 Domain decomposition into 8 processors of the generated 3D mesh. Various colors denote various polynomial orders of approximation from $p=1$ to $p=8$.

Demkowicz, L., 2002, 2D *hp*-Adaptive Finite Element Package (2D *hp* 90) Version 2.0, ICES Report 02-06, 1-72.

Demkowicz, L., 2004, Projection Based Interpolation, ICES Report 04-03, 1-22.

Demkowicz, L., Pardo, D., Rachowicz, W., 2002, 3D *hp*-Adaptive Finite Element Package (3D *hp* 90) Version 2.0, The Ultimate Data Structure for Three-Dimensional, Anisotropic *hp* Refinements, ICES Report 02-24, 1-54.

Kurtz, J., 2005, Fully Automatic *hp*-Adaptivity for Acoustic and Electromagnetic Scattering in Three Dimensions, Dissertation Proposal, The University of Texas at Austin.

Paszyński, M., Kurtz, J., Demkowicz, L., 2006, Parallel Fully Automatic *hp*-Adaptive 2D Finite Element Package, Computer Methods in Applied Mechanics and Engineering, 195, 7-8, 711-741.

Paszyński, M., Demkowicz, L., 2006, Parallel Fully Automatic *hp*-Adaptive 3D Finite Element Package, Engineering with Computers, in press.

Paszyński, M., Pardo, D., Torres-Verdin, C., Demkowicz, L., 2006, Fast Numerical Simulations of 3D DC Borehole Resistivity Measurements with a Parallel Self-Adaptive Goal-Oriented Finite Element Formulation, Sixth Annual Report of Joint Industry Research Consortium on Formation Evaluation, The University of Texas at Austin, August 16-18.

Pardo, D., Demkowicz, L., 2006, Integration of *hp*-adaptivity and a two-grid solver for elliptic problems, Computer Methods in Applied Mechanics and Engineering, 195, 7-8, 674-710.

Pardo, D., Demkowicz, L., Torres-Verdin, C., Paszynski, M., 2006, A Goal-Oriented *hp*-Adaptive Finite Element Strategy with Electromagnetic Applications. Part II: Electrodynamics, Computer Methods in Applied Mechanics and Engineering, 2006, in press.

Pardo, D., Paszyński, M., Torres-Verdin, C., Demkowicz, L., 2006, Numerical Simulations of 3D DC Borehole Resistivity Measurements using an *hp*-Adaptive Goal-Oriented Finite Element Formulation, Sixth Annual Report of Joint Industry Research Consortium on Formation Evaluation, The University of Texas at Austin, August 16-18.